State of stress in central and eastern North American seismic zones

Stephane Mazzotti[1] and John Townend[2]

[1]GEOLOGICAL SURVEY OF CANADA, NATURAL RESOURCES CANADA, P.O. BOX 6000, SIDNEY, BC V8L 4B2, CANADA *AND* SCHOOL OF EARTH AND OCEAN SCIENCES, UNIVERSITY OF VICTORIA, PO BOX 3065 STN CSC, VICTORIA, BC V8W 3V6, CANADA

[2]SCHOOL OF GEOGRAPHY, ENVIRONMENT, AND EARTH SCIENCES, VICTORIA UNIVERSITY OF WELLINGTON, P.O. BOX 600, WELLINGTON 6140, NEW ZEALAND

ABSTRACT

We use a Bayesian analysis to determine the state of stress from focal mechanisms in ten seismic zones in central and eastern North America and compare it with regional stress inferred from borehole measurements. Comparisons of the seismologically determined azimuth of the maximum horizontal compressive stress (S_{HS}) with that determined from boreholes (S_{HB}) exhibit a bimodal pattern: In four zones, the S_{HS} and regional S_{HB} orientations are closely parallel, whereas in the Charlevoix, Lower St. Lawrence, and Central Virginia zones, the S_{HS} azimuth shows a statistically significant 30°–50° clockwise rotation relative to the regional S_{HB} azimuth. This pattern is exemplified by the northwest and southeast seismicity clusters in Charlevoix, which yield S_{HS} orientations strictly parallel and strongly oblique, respectively, to the regional S_{HB} trend. Similar ~30° clockwise rotations are found for the North Appalachian zone and for the 2003 Bardwell earthquake sequence north of the New Madrid zone. The S_{HB}/S_{HS} rotations occur over 20–100 km in each seismic zone, but they are observed in zones separated by distances of up to 1500 km. A possible mechanism for the stress rotations may be the interaction between a long-wavelength stress perturbation source, such as postglacial rebound, and local stress concentrators, such as low-friction faults. The latter would allow low-magnitude (<10 MPa) postglacial rebound stresses to locally perturb the preexisting stress field in some seismic zones, whereas postglacial rebound stresses have little effect on the intraplate state of stress in general.

LITHOSPHERE; v. 2; no. 2; p. 76–83, Data Repository 2010020. doi: 10.1130/L65.1

INTRODUCTION

As in most continental intraplate regions, stress orientations in central and eastern North America are broadly homogeneous and consistent over 1000–5000 km spatial scales (e.g., Zoback and Zoback, 1980, 1991; Zoback, 1992a). East of the Cordillera deformation front, the main characteristic of the tectonic stress field is a NE-SW axis of maximum horizontal compressive stress (S_H), which is commonly attributed to far-field plate-boundary forces, and in particular to Mid-Atlantic Ridge push (Zoback, 1992a; Richardson, 1992). In a case study of 32 eastern North American earthquakes, Zoback (1992b) noted that most focal mechanisms were compatible with the regional stress field inferred from borehole data. However, five mechanisms suggested local stress perturbations, and two other events implied atypical frictional conditions (e.g., superlithostatic pore-fluid pressure).

The spatial distribution of earthquakes in central and eastern North America is largely associated with late Proterozoic Iapetus Rift structures (e.g., Adams and Basham, 1991; Johnston et al., 1994). As shown in Figure 1, the main concentrations of both small and large earthquakes lie along the rifted margin itself or failed rift arms. The Iapetus structures are typically reactivated under the present-day stress

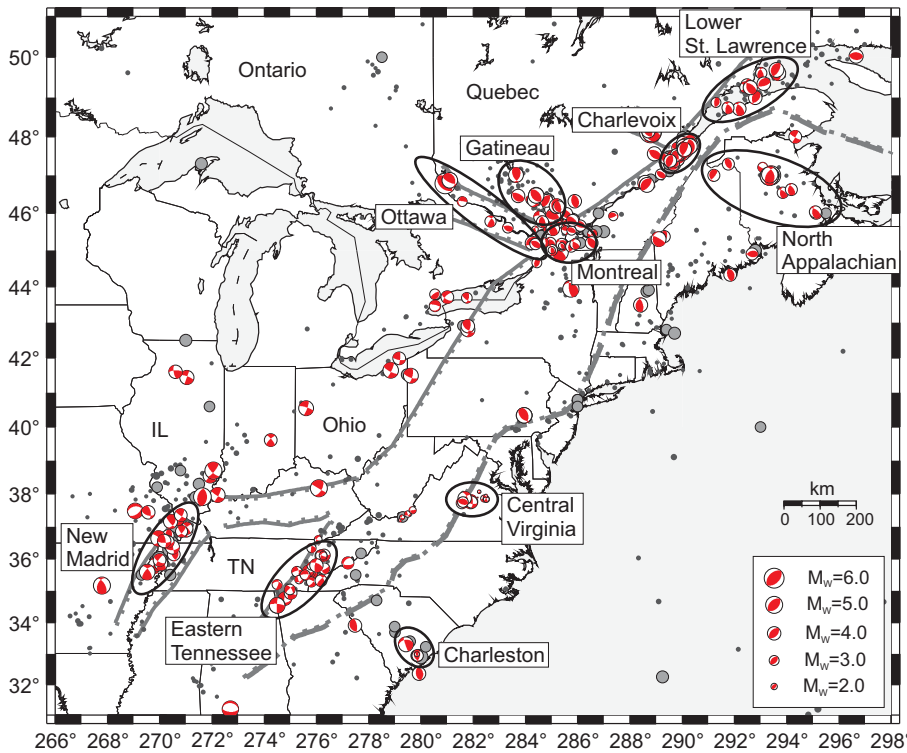

Figure 1. Central and eastern North America seismicity and Iapetus Rift structures. Dark- and light-gray dots show magnitude M ≥ 3 and M ≥ 5 earthquakes since 1973 (Geological Survey of Canada and U.S. Geological Survey catalogs). Focal mechanism (red) sources are given in the supplementary material (see text footnote 1). Thick gray barbed lines indicate the Iapetus rifted margin and failed rifts. The ten seismic zones discussed in the text are shown by solid ellipses.

field as thrust or strike-slip faults. Aside from this first-order correlation, rather little is known about the geological and geophysical conditions generating intraplate earthquakes and the associated hazard (cf. Stein and Mazzotti, 2007, and references therein). Thus, characterization of the regional stress field and local state of stress is essential for improving our understanding of the source of intraplate seismicity and better quantifying seismic hazard.

In this study, we analyze a newly compiled data set of focal mechanisms to estimate stress parameters and characterize the prevailing state of stress within ten of the main seismic zones of central and eastern North America. We compare our results with regional borehole stress information from the World Stress Map and Canadian Crustal Stress databases to determine the consistency of seismological and borehole estimates of the state of stress near the seismic zones and to elucidate potential stress perturbations associated with regionally elevated earthquake activity.

DATA SETS AND STRESS ESTIMATION TECHNIQUE

Focal Mechanisms

The earthquake focal mechanism data set is shown in Figure 1. (See supplementary material for references and focal mechanism octant plots.[1]) It constitutes mostly first-motion solutions complemented by a small number of moment tensors (~15% of the total). In most cases, a quality factor was provided in the original study in the form of a qualitative level (A–D) or a quantitative angular uncertainty. In order to obtain a coherent set of inversion results, we standardized these quality rankings by assigning small (±15°), medium (±25°), or large (±35°) uncertainties to each mechanism's strike, dip, and rake angles, which are assumed to be independent (cf. Walsh et al., 2009). In those cases in which the original study did not provide a quality level, we assigned an uncertainty level on the basis of the data-analysis description. In addition, focal mechanism uncertainties were adjusted on the basis of earthquake magnitudes to take into account the potentially higher uncertainty and lower quality of small-magnitude solutions: all $M < 2.5$ and $2.5 \le M < 3.5$ mechanisms were assigned large and medium uncertainties (±35° and ± 25°), respectively.

[1]GSA Data Repository Item 2010020, focal mechanism data set, octant plots, and Charlevoix stress analyses, is available at www.geosociety.org/pubs/ft2010.htm, or on request from editing@geosociety.org, Documents Secretary, GSA, P.O. Box 9140, Boulder, CO 80301-9140, USA.

We focus on ten of the main eastern North American seismic zones, which we define as areas encompassing more than five focal mechanisms within a distinct geological and seismological area (Fig. 1). The Lower St. Lawrence, Charlevoix, Montreal, and Eastern Tennessee zones are associated with the Iapetus rifted margin, and the Ottawa and New Madrid zones are associated with Iapetus failed rift arms (Adams and Basham, 1991; Wheeler, 1995). The Gatineau seismic zone may be related to the trace of the New England Seamount Chain hotspot (Adams and Basham, 1991). The North Appalachian, Central Virginia, and Charleston seismic zones are not affiliated with clear lithosphere-scale structures: in the first two, the seismicity occurs within the Appalachian formations that overlie rifted Grenville crust (Munsey and Bollinger, 1985; Adams and Basham, 1991). Other seismicity clusters can be identified in central and eastern North America, but the paucity of focal mechanisms precludes any stress analysis.

Seismological Stress Estimation

We used a Bayesian estimation technique (Arnold and Townend, 2007) to determine the set of stress parameters most consistent with the focal mechanisms in a given group. We weighted each focal mechanism by converting the aforementioned angular errors to a scalar Matrix Fisher concentration parameter (Equation A12 of Arnold and Townend, 2007). This approach yields a joint probability density function of the three angles specifying the principal stress axes' orientations and a single stress magnitude ratio parameter. Its principal advantages, in comparison with other stress estimation algorithms, are the incorporations of focal mechanism uncertainties, nodal plane ambiguity, and the weak constraint imposed on the stress tensor by any single focal mechanism. This last point is particularly important because it allows us to derive confidence intervals for the stress tensor parameters that take into account the degree of similarity between focal mechanisms within individual seismic zones (Arnold and Townend, 2007). As shown in the octant plots (supplementary material [see footnote 1]), the diversity of mechanisms can vary significantly between zones.

We computed the trend of the axis of maximum horizontal compressive stress (S_H) using the algorithm described by Lund and Townend (2007). Such a transformation is necessary when none of the three principal stresses is strictly vertical, and it enables all four determinable parameters to be amalgamated into a single, physically intuitive and readily illustrated parameter. This produces a probabilistic description of S_H from which we can compute the median trend and associated confidence intervals.

Borehole Stress Data

In order to perform a detailed comparison of our seismological stress estimates with borehole crustal stress measurements on a regional scale, we extracted stress magnitude and orientation data from the World Stress Map and the Canadian Crustal Stress databases (Zoback, 1992a; Adams, 1995; Heidbach et al., 2008). For each seismic zone, we calculated a weighted mean S_H orientation for borehole breakout and hydrofracture measurements with qualities of A, B, or C made at depths greater than 0.5 km within 250 km of each seismic zone. The weighted mean and its associated standard deviation were estimated by assigning weights of 3, 2, and 1 to the A, B, and C quality S_H measurements, respectively. In most cases, the borehole S_H data are located outside of the seismic zones and are unevenly distributed. Because of the strong regional coherence of the borehole stress orientations over distances of hundreds of kilometers (Zoback, 1992a), we assume that these 250 km S_H averages provide appropriate estimates of the regional stress orientation outside of the seismic zones.

RESULTS

Eastern North America

The results are shown in Figures 2 and 3 and listed in Table 1 in terms of median S_{HS} trend and 90% confidence interval ($90CI_S$); the subscript "S" is used to denote a seismological estimate. The 90% confidence interval is ~20°–40° in most cases. The Ottawa seismic zone stands out with a very large $90CI_S$ of 132°, indicating that the directions of the principal horizontal stresses are not constrained by this small data set (eight mechanisms, two of which have large uncertainties). The results for this zone are not used for further discussion.

In all but one case, the estimated S_{HS} orientation lies in the NE-SW quadrant, roughly parallel to the general S_{HB} trend inferred from borehole measurements (Fig. 3); the subscript "B" is used to denote a borehole estimate. For the New Madrid, Eastern Tennessee, Montreal, and Gatineau seismic zones, the median seismological and average borehole S_H orientations (S_{HS} and S_{HB}, respectively) are consistent to within 5°–15°, well within the respective 90% confidence intervals. The lack of borehole S_{HB} data within 250 km of the Charleston seismic zone precludes a direct comparison with the S_{HS} orientation. However, the nearest S_{HB} measurement (C quality at

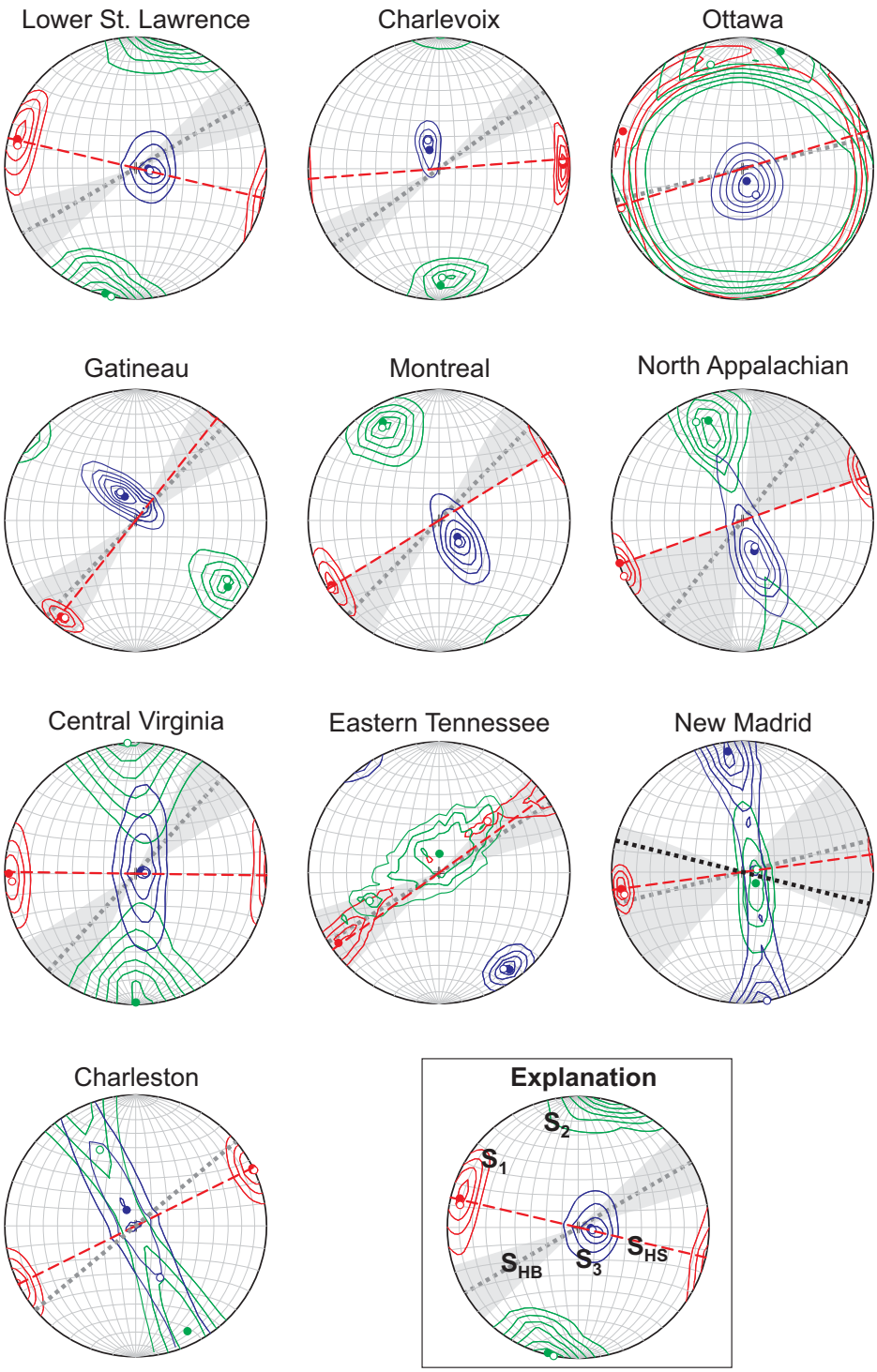

Figure 2. State of stress in seismic zones. Lower-hemisphere stereonets show the posterior distributions of the principal stress axes (S_1—red, S_2—green, S_3—blue). Dashed red lines indicate the median orientation of the seismologically determined maximum horizontal compressive stress S_{HS}. Dotted gray lines and gray angular sectors indicate the average and 90% confidence region of the maximum horizontal compressive stress from borehole data S_{HB} (Table 1). New Madrid: The black dotted line shows the S_1 orientation for the Bardwell earthquake sequence (Horton et al., 2005).

255 km) has an orientation that lies within the 90% confidence interval of S_{HS} (Fig. 2). For the North Appalachian seismic zone, the median S_{HS} and average S_{HB} values differ by 33°, but the 90% confidence intervals overlap by 13° (Fig. 2). The three remaining seismic zones (Central Virginia, Lower St. Lawrence, and Charlevoix) show statistically significant differences between S_{HS} and S_{HB} azimuths and are discussed in more detail in the following sections.

Central Virginia Seismic Zone

The state of stress in the Central Virginia seismic zone was determined by the focal mechanisms of 11 small earthquakes (M < 3) recorded during 4 yr in the early 1980s (Munsey and Bollinger, 1985), complemented by two M ~4 earthquakes that occurred in 2003. These events all occurred at regionally typical depths shallower than ~15 km within the allochthonous, thrust-faulted, Appalachian formations that override the Precambrian Grenville basement (Bollinger et al., 1985; Munsey and Bollinger, 1985).

The S_{HS} orientation is rotated 48° clockwise with respect to the regional borehole S_{HB} trend, and the 90% confidence intervals of S_{HS} and S_{HB} are separated by 13° (Table 1; Fig. 2), indicating that the two estimates are significantly distinct. Using the same data set, excluding the 2003 events, Kim and Chapman (2005) inferred a slightly larger clockwise rotation of S_{HS} relative to S_{HB} (~68°), with an azimuth and plunge of N133° and 14°SE for the S_1 axis (cf. N086° and 7°W for our results; Fig. 2). The difference in orientation and plunge of S_1 between the two analyses may be in part due to the difference in the stress inversion technique (Bayesian versus grid-search). Alternatively, the difference in results may reflect the small difference in the data sets in relation to the complexity of the seismological state of stress in the Central Virginia seismic zone. The 13 focal mechanisms have P axis orientations in both NE-SW and NW-SE directions, suggesting that the stress regime may change from mainly thrust to mainly strike slip with depth (Munsey and Bollinger, 1985).

Lower St. Lawrence Seismic Zone

The Lower St. Lawrence seismic zone is delineated by pronounced microseismicity located mainly beneath the St. Lawrence River (Fig. 1) (Adams and Basham, 1991). The best-constrained hypocenters place the earthquakes between 7 and 25 km depth, within the rifted Precambrian Grenville basement and well below the overthrust Appalachian formations (Adams and Basham, 1991; Lamontagne et al., 2003).

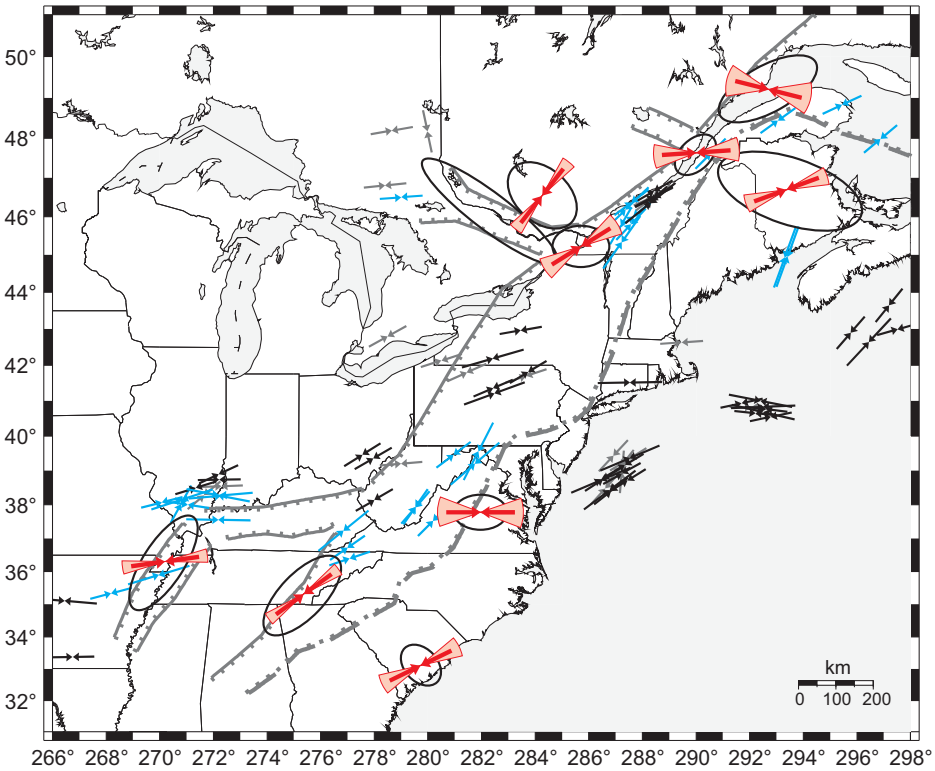

Figure 3. Eastern North America maximum horizontal compressive stress. Solid and gray arrows indicate S_{HB} orientation from borehole observations (A and B–C quality, respectively). Blue arrows indicate borehole observations used in calculating the regional average within 250 km of the seismic zones (solid ellipses). Red arrows and angular sectors indicate S_{HS} orientation from focal mechanism inversion (median and 90% range, Table 1).

TABLE 1. STRESS INVERSION RESULTS VERSUS LOCAL BOREHOLE STRESS ORIENTATION

Seismic zone	Seismological stress				Borehole stress		
	N_S	S_{HS} (°)	$90CI_S$ (°)	R	N_B	S_{HB} (°)	$90CI_B$ (°)
Lower St. Lawrence	12	104 (R)	081–124	0.4	2	060	46–73
Charlevoix	60	086 (R)	069–101	0.3	12	054	43–65
Charlevoix NW	25	055 (R)	035–074	0.2	12	054	43–65
Charlevoix SE	35	101 (R)	086–114	0.4	12	054	43–65
Gatineau	19	038 (R)	029–048	0.8	6	043	28–58
Ottawa	8	078 (R)	001–133	0.3	1	086	—
Montreal	21	058 (R)	043–073	0.4	7	044	30–59
North Appalachian	12	070 (R)	059–083	0.6	5	038	5–71
Central Virginia	13	090 (R)	071–111	0.7	6	042	26–58
East Tennessee	26	054 (S)	046–063	0.2	3	058	43–73
New Madrid	18	082 (S)	073–091	0.9	10	076	41–111
Charleston	11	064 (S)	050–077	1.0	1	040*	—

Note: N_S—number of focal mechanisms; S_{HS} and $90CI_S$—median and 90% confidence interval azimuth of the axis of maximum horizontal compressive stress (R—reverse, S—strike-slip); R—median stress ratio $(S_1 - S_2)/(S_1 - S_3)$; N_B—number of borehole data; S_{HB} and $90CI_B$—weighted average and 90% confidence interval azimuth of the borehole axis of maximum horizontal compression within 250 km of the seismic zone.
*Based on nearest borehole at 255 km.

Although tentative correlations have been made between the earthquakes and the Iapetus Rift faults, most of the seismicity appears to occur within fractured volumes of the rift system rather than on the main rift faults themselves (Lamontagne et al., 2003).

The S_{HS} orientation is rotated 44° clockwise compared to the regional borehole stress orientation S_{HB} (Table 1; Fig. 2). The 90% confidence intervals for the two estimates are separated by 8°, indicating a statistically significant difference. There are two important caveats with regard to this observation: (1) the S_{HB} orientation and standard error are only based on two B quality data points (individual azimuths of 54° and 65°; Fig. 3); and (2) the S_{HS} orientation is only defined by 12 mechanisms, exhibiting a relatively low diversity and hence yielding a relatively large $90CI_S$ value. Notwithstanding these points, the seismological versus borehole stress rotation appears to be robust, and the borehole S_{HB} orientation is similar to the general direction for eastern Canada (Fig. 3). The seismological S_{HS} value is stable for several tested combinations of eight or more (out of 12) mechanisms and yields a S_{HS} orientation between N100° and N120°, in all cases strongly oblique to the regional borehole data.

Charlevoix Seismic Zone

The Charlevoix seismic zone is one of the historically most active earthquake concentrations in eastern North America, with five $M \geq 6$ earthquakes since 1663 (Lamontagne, 1987; Adams and Basham, 1991). Most earthquakes occur between 5 and 25 km depth beneath the St. Lawrence River. The main geological structures are related to the ca. 1100 Ma Grenville orogeny, ca. 650 Ma Iapetus rifting, ca. 450 Ma Appalachian orogeny, and a large meteor impact ca. 350 Ma. Using remote-sensing, seismic, and potential field data, Lamontagne et al. (2000) identified the Saint-Laurent and Charlevoix faults (Fig. 4) as the main Iapetus Rift faults and the principal structures in the seismic zone.

No clear association can be found between the seismicity and the main fault structures (e.g., Lamontagne et al., 2000), but a first-order NW-SE clustering pattern is apparent in the earthquakes' epicenters. As shown in Figure 4, a largely aseismic, ~5-km-wide zone separates two distinct microseismicity clusters to the southeast (mostly beneath the river) and the northwest (mostly beneath the north shore; Anglin and Buchbinder, 1981). This gap coincides with an elongated high-seismic-velocity body (Vlahovic et al., 2003) and with the location of the Saint-Laurent fault (Fig. 4, cross section).

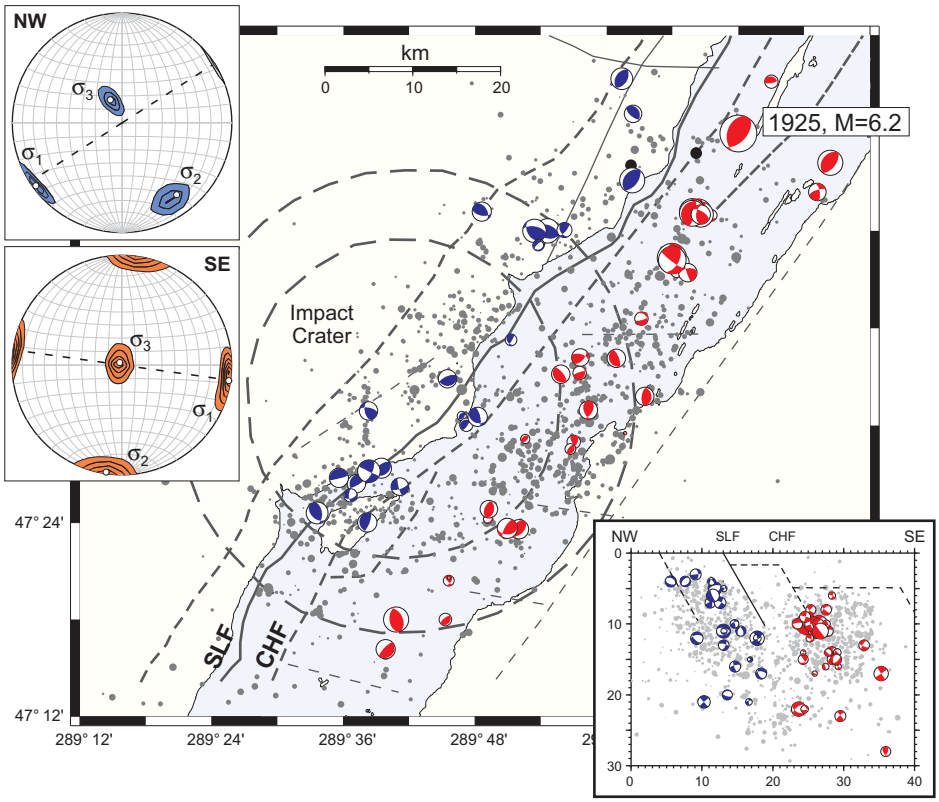

Figure 4. Charlevoix maximum horizontal compressive stress. Earthquakes and focal mechanisms are as in Figure 1. Solid and dashed lines show Iapetus Rift faults and impact crater structure (Lamontagne et al., 2000). SLF—Saint-Laurent fault; CHF—Charlevoix fault. Lower-right insert shows a NW-SE depth cross section. The upper-left insert shows stereonets of the state of stress from inversion of focal mechanisms to the northwest (blue) and southeast (red) of the Saint-Laurent fault.

Analysis of the 60 focal mechanisms in the Charlevoix seismic zone yields a S_{HS} orientation of N086°, rotated 32° clockwise relative to the regional S_{HB} from nearby boreholes (Table 1; Fig. 2). The 90% confidence intervals for the two estimates are distinct by 4°. The large number of focal mechanisms allows us to test for spatial variations in stress orientations amongst subsets of events. The most significant difference in S_{HS} orientation exists between the focal mechanism clusters to the southeast and northwest of the Saint-Laurent fault (Fig. 4). For the northwest group, S_{HS} is oriented N055°, parallel to the regional borehole data, whereas S_{HS} for the southeast group is oriented N101° and rotated clockwise by 47° compared to the borehole trend (Table 1; Fig. 4). This rotation is significant at the 90% confidence level, with a separation of 21° between the seismological and borehole confidence intervals. Various earthquake grouping and inversion tests (supplementary material [see footnote 1]) indicate that the NW-SE clustering is the grouping associated with the most significant rotation.

The 1925 Charlevoix M = 6.2 earthquake ruptured a steeply dipping thrust fault striking parallel to the regional S_H orientation (Bent, 1992; Fig. 4). The rotated S_{HS} observed for the southeast side of the Charlevoix seismic zone is more compatible than the regional S_H direction with the focal mechanism of the 1925 event, as well as with numerous smaller thrust events that have fault planes striking NE-SW.

DISCUSSION

Consistency and Extent of Stress Rotations

Out of the ten seismic zones addressed in this study, the Central Virginia, Lower St. Lawrence, and Charlevoix seismic zones each show a 30°–50° clockwise rotation of the seismic S_{HS} orientation relative to the regional borehole S_{HB} orientation that is significant at the 90% confidence level. A similar clockwise rotation of 32° is observed for the North Appalachian seismic zone, albeit with a 12° overlap of the seismological and borehole 90% confidence intervals (Fig. 2). Although not statistically significant, that result is worth noting in comparison with the 48° clockwise rotation observed in the Central Virginia seismic zone: both seismic zones exhibit clusters of earthquakes confined to the shallow (<15 km) Appalachian formations that override the deeper Grenville basement (Bollinger et al., 1985; Adams and Basham, 1991).

A similar, although slightly smaller, clockwise rotation can be deduced for the 2003 M = 4.0 Bardwell earthquake sequence north of the New Madrid seismic zone. For the main shock and aftershock sequence, Horton et al. (2005) derived a S_1 orientation of N104° with an uncertainty of approximately ±20°. Assuming that $S_{HS} = S_1$, this result indicates a clockwise rotation of 20°–30° compared to our median estimates of S_{HS} for the New Madrid focal mechanisms (excluding the Bardwell sequence) and S_{HB} from nearby borehole data (Table 1; Fig. 2). Although not statistically significant, this apparent rotation suggests that large variations in stress orientation can occur over a distance of ~40 km in the New Madrid–Wabash Valley area (Horton et al., 2005), similar to the ~20 km distance that separates the two seismic clusters in the Charlevoix seismic zone.

It is important to consider whether the apparent stress rotations are artifacts stemming from the comparison between relatively shallow borehole data (0.5–2 km) and deeper seismicity (1–30 km). Vertical variations in stress orientations have been reported over depth intervals of 100–1000 m in individual boreholes (e.g., Hickman and Zoback, 2004), but in general, deep borehole- and earthquake-determined stress orientations are similar and can be jointly accounted for in terms of, for instance, dynamical modeling results (e.g., Townend and Zoback, 2004). Moreover, the eastern and western Charlevoix results are based on earthquakes at comparable depths. Hence, we consider it unlikely that the observed rotations are depth-related artifacts.

Overall, therefore, we find that the angular difference between S_{HS} and S_{HB} exhibits a bimodal pattern: four seismic zones exhibit good agreement between seismological and borehole estimates of the S_H orientation (Gatineau, Montreal, Eastern Tennessee, and New Madrid), and five imply 30°–50° clockwise rotations of the seismological S_{HS} relative to the regional borehole S_{HB} (Lower St. Lawrence, Charlevoix, Central Virginia, and, to a lesser extent, North Appalachian and Bardwell–northern New Madrid). In the case of the Lower St. Lawrence, Central Virginia, and North Appalachian, the rotation between S_{HS} inside the seismic zone and S_{HB} outside the seismic zone occurs over distances of 50–100 km (Fig. 3). For Charlevoix and Bardwell–northern New Madrid, the rotation occurs over 20–40 km (Fig. 4). In the following section, we consider the magnitude and potential causes of the stress perturbation required to

account for the 30°–50° clockwise rotation of the horizontal principal stresses over such short distances.

Magnitude of the Stress Perturbations

In order to obtain a first-order estimate of the stress perturbation causing the observed rotations, we consider the model of Sonder (1990) and Zoback (1992a). In this model, the orientation of the maximum horizontal compressive stress (represented here by S_{HS}) in the vicinity of a major structure can be calculated in terms of a regional stress orientation (represented here by S_{HB}) and a uniaxial stress perturbation (S_L) orthogonal to the strike of the structure. We assume that, for the Charlevoix, Lower St. Lawrence, and Central Virginia seismic zones, the stress responsible for the local rotation is perpendicular to the average local Iapetus Rift direction (Fig. 1). With this assumption, the magnitude of the uniaxial stress perturbation S_L is found using Equation 8 of Zoback (1992a) to be 80%–110% that of the regional horizontal differential stress (i.e., $[S_H - S_h]/S_L \sim 0.8–1.1$; Table 2).

Deep intraplate borehole data from a number of locations worldwide reveal that at depths of as much as 8 km, the crust is in a state of stress consistent with incipient frictional failure given coefficients of friction $\mu \approx 0.6–1.0$ and the observed near-hydrostatic pore-fluid pressures ($\lambda \approx 0.4$; Townend and Zoback, 2000). Similarly, stress magnitude data from boreholes in central and eastern North America (Adams and Bell, 1991; Adams, 1995; Heidbach et al., 2008) show a relationship between differential stress ($S_1 - S_3$) and effective mean stress that is consistent with incipient frictional failure for coefficients of friction $\mu > 0.5$ (Fig. 5). Also illustrated in Figure 5, a histogram of stress ratio measurements from the same boreholes exhibits a pronounced peak at $0.5 \le R_B \le 0.8$ and mean of $R_B = 0.6$, with few values smaller than 0.4. The majority of these borehole stress measurements are located in the Canadian Shield, west and north of the main seismic zones. Thus, they may be considered as constituting a reference state of stress for the continental crust outside of seismically active regions.

If we assume that the stress magnitude parameters in each seismic zone are similar to those in intraplate continental crust as a whole ($\mu = 0.8$, $\lambda = 0.4$, $R = 0.6$, $\rho = 2700$ kg m^{-3}; see Appendix A for details), the differential stress in the horizontal plane at a mid-seismogenic zone depth of 8 km is $S_H - S_h = S_1 - S_2 \approx 250$ MPa for a reverse stress state, and $S_H - S_h = S_1 - S_3 \approx 160$ MPa for a strike-slip stress state. This analysis suggests that a local stress perturbation S_L of comparable magnitude is required to locally reorient S_{HB} by 30°–50°, as implied by the Lower St. Lawrence, Charlevoix, and Central Virginia stress orientation results.

Such high stress magnitudes clearly depend on the assumed friction coefficient and the fluid pressure regime. If we assume that either a low friction coefficient ($\mu = 0.1$) or a near-lithostatic pore-fluid pressure ($\lambda \approx 0.9$) prevails in the seismic zones, the horizontal differential stress and the corresponding stress perturbation S_L would be of the order of only ~20–40 MPa. However, the low ambient stress magnitudes implied by those parameters contrast markedly with the values thought to characterize aseismic or low-seismicity intraplate continental crust as a whole, as outlined herein (Fig. 5).

Potential Sources of the Stress Perturbations

The consistency of the 30°–50° clockwise stress rotations observed from the St. Lawrence valley to the central Appalachians (and possibly to the New Madrid–Wabash Valley) suggests a similar mechanism or source for seismic zones separated by large distances. The calculations discussed in the previous section imply a stress perturbation at mid-seismogenic depths of 160–250 MPa (in a representative high-friction, low-fluid-pressure case) or 20–40 MPa (low friction or high fluid pressure) and a maximum horizontal stress S_L trending approximately N115°–135° (Table 2).

Various mechanisms have been proposed as potential sources of local and regional stress perturbations, including topography, crustal density anomalies, fault intersections, flexure under local loads (e.g., sedimentary basins), and postglacial rebound (e.g., Stein et al., 1989; Talwani, 1988; Zoback, 1992a; Assameur and Mareschal, 1995). Most of these mechanisms account for stress perturbations of at most a few tens of megapascals and would only result in significant horizontal stress rotations if prevailing horizontal stresses were at the low end of stress levels calculated here. Flexural stresses may reach several hundred megapascals under sediment loads of 10 km thickness (Stein et al., 1989), but such conditions do not appear

TABLE 2. STRESS PERTURBATION MAGNITUDE AND ORIENTATION

Seismic zone	Structure (°)	S_{HB} (°)	S_{HS} (°)	θ (°)	γ (°)	$(S_H - S_h)/S_L$	S_L (°)
Lower St. Lawrence	045	060	104	15	44	0.88	135
Charlevoix	035	054	086	19	32	1.09	125
Central Virginia	027	042	090	15	48	0.81	117

Note: Structure—average azimuth of primary regional structural direction; S_{HS} and S_{HB}—azimuth of axis of maximum horizontal compressive stress from seismic inversion and borehole data (cf. Table 1). $\theta = S_{HB} -$ structure; $\gamma = S_{HS} - S_{HB}$. $(S_H - S_h)/S_L$ is ratio of local horizontal differential stress to stress perturbation (S_L, cf. text and Sonder, 1990). S_L—azimuth of stress perturbation.

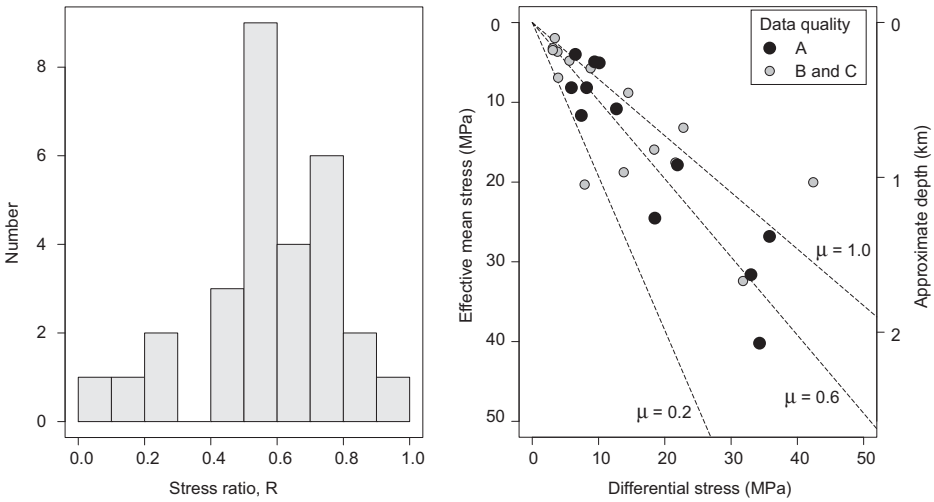

Figure 5. Stress ratio and differential stress from borehole data. Left: Histogram of stress ratio R = $(S_1 - S_3)/(S_2 - S_3)$ from A, B, and C quality borehole stress measurements deeper than 0.5 km in eastern North America. Right: Differential stress ($S_1 - S_3$) versus effective mean stress (mean stress minus pore fluid pressure) from borehole stress measurements deeper than 0.1 km of quality A (open circles) and B or C (solid circles) in eastern North America.

applicable to continental seismic zones. Similarly, large crustal density anomalies have been demonstrated to produce stress perturbations of as much as ~200 MPa and rotations of up to 90° (Zoback and Richardson, 1996). However, gravity and seismic velocity data do not indicate the presence of widespread high-density anomalies associated with the Iapetus Rift structures in the Charlevoix and Lower St. Lawrence seismic zones (Lamontagne et al., 2000, 2003).

One possible mechanism by which consistent local stress perturbations may be generated over large distances is the concentration of postglacial rebound stresses by local zones of weakness, perhaps including low-friction faults. Postglacial rebound stresses show a strong spatial coherence over distances of thousands of kilometers, but they are typically smaller than ~10 MPa (e.g., Wu and Hasegawa, 1996). However, the presence of a "weak zone" in the lithosphere, such as low upper-mantle viscosity or a low-friction fault in the crust, can result in stress amplifications by a factor of 5–10 with respect to homogeneous lithosphere models (e.g., Grollimund and Zoback, 2001; Wu and Mazzotti, 2007). In such cases, the modulation of large-scale, small-amplitude postglacial rebound stresses by local zones of weakness could produce perturbations that are coherent over large distances but only affect those areas with locally reduced horizontal differential stress levels. In other words, postglacial rebound stresses may be high enough to reorient the local stress field surrounding faults with low friction or other properties that maintain ambient stress at levels lower than in the "typical low-seismicity" continental intraplate crust.

The St. Lawrence Valley may provide possible examples of this mechanism. In both the Lower St. Lawrence and Charlevoix seismic zones, the estimated S_{HS} orientation is strongly oblique to the regional S_{HB} orientation derived from borehole data located 30–100 km outside the seismic zones (Fig. 3). In Charlevoix, the relationships between the seismicity distribution and geological structures jointly suggest that the main rift faults may have unusually low friction ($\mu \sim 0.1$; Baird et al., 2009). Recent models of postglacial rebound stress and strain that incorporate a weak zone in the lithosphere beneath the St. Lawrence Valley show a significant amplification and clockwise rotation of the postglacial rebound stresses directly above the weak zone (Wu and Mazzotti, 2007). The resulting postglacial rebound horizontal stress and strain orientations are nearly parallel to our estimated S_{HS} orientation and to the maximum horizontal contraction rate measured by global positioning system in the Charlevoix and Lower St. Lawrence seismic zones (Mazzotti et al., 2005, 2006).

CONCLUSIONS

(1) Comparisons of the axis of maximum horizontal compressive stress determined from earthquake focal mechanisms in seismic zones (S_{HS}) and from borehole data near but outside the seismic zones (S_{HB}) reveal a bimodal pattern: S_{HS} and S_{HB} are closely parallel in four seismic zones (Gatineau, Montreal, Eastern Tennessee, and New Madrid); in three other zones (Lower St. Lawrence, Charlevoix, and Central Virginia), S_{HS} is rotated 30°–50° clockwise compared to S_{HB}; two other zones (North Appalachian and Bardwell–northern New Madrid) show indications of similar clockwise rotations but at a low confidence level.

(2) The observed S_{HS} versus S_{HB} rotations are similar in both sense and magnitude in seismic zones separated by up to ~1500 km.

(3) The observed S_{HS} versus S_{HB} rotations occur over distances of no more than 50–100 km. In two cases (SE versus NW Charlevoix and Bardwell versus New Madrid), the rotation appears to occur over a distance of 20–50 km.

(4) With respect to a simple model of stress rotations near structural boundaries, the observed S_{HS} versus S_{HB} rotations imply a local stress perturbation of 160–250 MPa at a representative depth of 8 km. This assumes that the crust in the seismic zones is in a state of stress similar to that of "typical, low-seismicity" continental crust as a whole, namely, incipient frictional failure with coefficients of friction $\mu \approx 0.6$–1.0 and near-hydrostatic pore-fluid pressures. If the seismic zones were characterized by either a very low coefficient of friction ($\mu = 0.1$) or a near-lithostatic pore-fluid pressure, the required stress perturbation according to the model used here would be only 20–40 MPa.

(5) Local stress perturbations associated with fault intersections or large density anomalies could be sufficiently large (hundreds of megapascals) to account for the observed rotations, but their short wavelength (~10–100 km) cannot explain similar S_{HS} rotations over 1500 km (point 2).

(6) Long-wavelength (hundreds of kilometers) stress perturbation mechanisms such as topography, basin flexure, and postglacial rebound are typically associated with stress magnitudes of the order of tens of megapascals and thus cannot straightforwardly account for the observed S_{HS} rotations if midcrustal stress magnitudes are of the order of hundreds of megapascals (point 4).

(7) A possible mechanism for similar stress perturbations over large distances is the concentration of postglacial rebound stresses by local zones of weakness, such as low-friction faults. This would result in long-wavelength perturbations affecting only the weak zones. The Lower St. Lawrence and Charlevoix seismic zones may be examples of such mechanism, where the S_{HS} orientation in the seismic zones is parallel to that predicted by postglacial rebound models that incorporate a local weak zone (Mazzotti et al., 2006).

APPENDIX A. STRESS MAGNITUDES

To estimate the regional stress magnitudes, we adopt the critically stressed crust model of Townend and Zoback (2000) in which the state of stress in the crust is controlled by optimally oriented Andersonian faults on the brink of frictional failure equilibrium. In this case, the maximum and minimum effective stresses, $S_1 - P_f$ and $S_3 - P_f$, are related by:

$$\frac{S_1 - P_f}{S_3 - P_f} = \left(\sqrt{\mu^2 + 1} + \mu\right)^2 \equiv F, \qquad \text{(A1)}$$

where P_f is the pore-fluid pressure, and μ the coefficient of friction (see Zoback and Townend, 2001, and references therein).

In normal, strike-slip, and reverse stress states, the effective vertical stress S_V is:

$$S_v = (1-\lambda)\,pgz = \begin{cases} S_1 & \text{normal} \\ S_2 & \text{strike-slip} \\ S_3 & \text{reverse} \end{cases}, \qquad \text{(A2)}$$

where ρ is the average crustal density, g is the gravitational acceleration, z is the depth, and $\lambda = P_f/S_v$ is the pore-fluid factor. In each case, we can express all three principal stresses in terms of the vertical stress S_V and the differential stress $\Delta S = S_1 - S_3$, and solve Equation A1 to obtain ΔS as a function of depth and the frictional parameter F. This yields:

$$\Delta S = pgz(\lambda - 1)(1 - F) \times \begin{cases} 1/F & \text{normal} \\ 1/\left(R + (1-R)F\right) & \text{strike-slip} \\ 1 & \text{reverse} \end{cases}, \qquad \text{(A3)}$$

where the stress ratio

$$R = \frac{S_1 - S_2}{S_1 - S_3} = \frac{S_1 - S_2}{\Delta S} \qquad \text{(A4)}$$

appearing in the strike-slip case is used to explicitly relate the intermediate principal stress to the differential stress. Expressions A2–A4 can be used to compute all three principal stress magnitudes and hence, given the orientation of the maximum horizontal stress, fully determine the stress tensor.

ACKNOWLEDGMENTS

We thank John Adams and Mark Zoback for ongoing discussions about eastern North America stress and seismicity, John Cassidy and Roy Hyndman for comments on a preliminary version of the manuscript, and Björn Lund for very detailed input during the review process. Allison

Bent, Shutien Ma, Pradeed Talwani, and Maurice Lamontagne provided focal mechanisms and data assistance, and Ikuko Wada helped with an early analysis. This is Geological Survey of Canada contribution 20080471.

REFERENCES CITED

Adams, J., 1995, The Canadian Crustal Stress Database—A compilation to 1994: Geological Survey of Canada Open-File 3122, 437 p.

Adams, J., and Basham, P.W., 1991, The seismicity and seismotectonics of eastern Canada, *in* Slemmon, B., et al., eds., The Geology of North America, Decade Map Volume 1, Neotectonics of North America: Boulder, Colorado, Geological Society of America, p. 261–276.

Adams, J., and Bell, J.S., 1991, Crustal stress in Canada, *in* Slemmon, B., et al., eds., The Geology of North America, Decade Map Volume 1, Neotectonics of North America: Boulder, Colorado, Geological Society of America, p. 367–386.

Anglin, F., and Buchbinder, G., 1981, Microseismicity in the mid–St. Lawrence Valley Charlevoix zone, Quebec: Bulletin of the Seismological Society of America, v. 71, p. 1553–1560.

Arnold, R., and Townend, J., 2007, A Bayesian approach to estimating tectonic stress from seismological data: Geophysical Journal International, v. 170, p. 1336–1356, doi: 10.1111/j.1365-246X.2007.03485.x.

Assameur, D.M., and Mareschal, J.C., 1995, Stress induced by topography and crustal density heterogeneities: Implication for the seismicity of southeastern Canada: Tectonophysics, v. 241, p. 179–192, doi: 10.1016/0040-1951(94)00202-K.

Baird, A.F., McKinnon, S.D., and Godin, L., 2009, Stress channeling and partitioning of seismicity in the Charlevoix seismic zone, Quebec, Canada: Geophysical Journal International, v. 179, p. 559–568, doi: 10.1111/j.1365-246X.2009.04275.x.

Bent, A.L., 1992, A re-examination of the 1925 Charlevoix, Quebec, earthquake: Bulletin of the Seismological Society of America, v. 82, p. 2097–2113.

Bollinger, G.A., Chapman, M.C., Sibol, M.S., and Costain, J.K., 1985, Analysis of earthquake focal depths in the southeastern U.S.: Geophysical Research Letters, v. 12, p. 785–788, doi: 10.1029/GL012i011p00785.

Grollimund, B., and Zoback, M.D., 2001, Did deglaciation trigger New Madrid seismicity?: Geology, v. 29, p. 175–178, doi: 10.1130/0091-7613(2001)029<0175:DDTISI>2.0.CO;2.

Heidbach, O., Tingay, M., Barth, A., Reinecker, J., Kurfeß, D., and Müller, B., 2008, The Release 2008 of the World Stress Map: http://www.world-stress-map.org (June 2009).

Hickman, S., and Zoback, M.D., 2004, Stress orientations and magnitudes in the SAFOD pilot hole: Geophysical Research Letters, v. 31, L15S12, doi: 10.1029/2004GL020043.

Horton, S.P., Kim, W.Y., and Withers, M., 2005, The 6 June 2003 Bardwell, Kentucky, earthquake sequence: Evidence for a locally perturbed stress field in the Mississippi embayment: Bulletin of the Seismological Society of America, v. 95, p. 431–445, doi: 10.1785/0120040052.

Johnston, A.C., Coppersmith, K.J., Kanter, L.R., and Cornell, C.A., 1994, The earthquakes of stable continental regions: Assessment of large earthquake potential, *in* Schneider, J.F., ed., Electronic Power Research Institute Report TR-102261: Palo Alto, California, Electronic Power Research Institute, 309 p.

Kim, W.-Y., and Chapman, M., 2005, The 9 December 2003 Central Virginia earthquake sequence: A compound earthquake in the Central Virginia seismic zone: Bulletin of the Seismological Society of America, v. 95, p. 2428–2445, doi: 10.1785/0120040207.

Lamontagne, M., 1987, Seismic activity and structural features in the Charlevoix region, Quebec: Canadian Journal of Earth Sciences, v. 24, p. 2118–2129, doi: 10.1139/e87-202.

Lamontagne, M., Keating, P., and Toutin, T., 2000, Complex faulting confounds earthquake research in the Charlevoix seismic zone, Québec: Eos (Transactions, American Geophysical Union), v. 81, no. 26, p. 289, doi: 10.1029/00EO00213.

Lamontagne, M., Keating, P., and Perreault, S., 2003, Seismotectonic characteristics of the Lower St. Lawrence seismic zone, Quebec: Insights from geology, magnetics, gravity, and seismics: Canadian Journal of Earth Sciences, v. 40, p. 317–336, doi: 10.1139/e02-104.

Lund, B., and Townend, J., 2007, Calculating horizontal stress orientations with full or partial knowledge of the tectonic stress tensor: Geophysical Journal International, v. 170, p. 1328–1335, doi: 10.1111/j.1365-246X.2007.03468.x.

Mazzotti, S., James, T.S., Henton, J., and Adams, J., 2005, GPS crustal strain, postglacial rebound, and seismicity in eastern North America: The Saint Lawrence Valley example: Journal of Geophysical Research, v. 110, B11301, doi: 10.1029/2004JB003590.

Mazzotti, S., Wu, P., Wada, I., Adams, J., and Bent, A., 2006, Role of plate tectonic and postglacial rebound forces in the present-day state of stress and fault reactivation along the St. Lawrence and Ottawa Valleys: Geological Association of Canada Meeting Abstracts, v. 31, p. 99.

Munsey, J.W., and Bollinger, G.A., 1985, Focal mechanism analyses for Virginia earthquakes: Bulletin of the Seismological Society of America, v. 75, p. 1613–1636.

Richardson, R.M., 1992, Ridge forces, absolute plate motion, and the intraplate stress field: Journal of Geophysical Research, v. 97, no. B8, p. 11,739–11,748, doi: 10.1029/91JB00475.

Sonder, L.J., 1990, Effects of density contrasts on the orientation of stresses in the lithosphere: Relation to principal stress directions in the Transverse Ranges, California: Tectonics, v. 9, p. 761–771, doi: 10.1029/TC009i004p00761.

Stein, S., and Mazzotti, S., eds., 2007, Continental Intraplate Earthquakes: Science, Hazard, and Policy Issues: Boulder, Colorado, Geological Society of America Special Paper 425, 402 p.

Stein, S., Cloetingh, S., Sleep, N.H., and Wortel, R., 1989, Passive margin earthquakes, stresses and rheology, *in* Gregersen, S., and Basham, P., eds., Earthquakes at North-Atlantic Passive Margins: Neotectonics and Postglacial Rebound: NATO ASI Series C: Boston Massachusetts, Kluwer, p. 231–259.

Talwani, P., 1988, The intersection model for intraplate earthquakes: Seismological Research Letters, v. 59, p. 305–310.

Townend, J., and Zoback, M.D., 2000, How faulting keeps the crust strong: Geology, v. 28, p. 399–402, doi: 10.1130/0091-7613(2000)28<399:HFKTCS>2.0.CO;2.

Townend, J., and Zoback, M.D., 2004, Regional tectonic stress near the San Andreas fault in central and southern California: Geophysical Research Letters, v. 31, L15S11, doi: 10.1029/2003GL018918.

Vlahovic, G., Powell, C., and Lamontagne, M., 2003, A three-dimensional P wave velocity model for the Charlevoix seismic zone, Quebec, Canada: Journal of Geophysical Research, v. 108, no. B9, p. 2439, doi: 10.1029/2002JB002188.

Walsh, D., Arnold, R., and Townend, J., 2009, A Bayesian approach to determining and parameterizing earthquake focal mechanisms: Geophysical Journal International, v. 176, p. 235–255, doi: 10.1111/j.1365-246X.2008.03979.x.

Wheeler, R.L., 1995, Earthquakes and the cratonward limit of lapetan faulting in eastern North America: Geology, v. 23, p. 105–108, doi: 10.1130/0091-7613(1995)023<0105:EATCLO>2.3.CO;2.

Wu, P., and Hasegawa, H., 1996, Induced stresses and fault potential in eastern Canada due to a realistic load: A preliminary analysis: Geophysical Journal International, v. 127, p. 215–229, doi: 10.1111/j.1365-246X.1996.tb01546.x.

Wu, P., and Mazzotti, S., 2007, Effects of a lithospheric weak zone on postglacial seismotectonics in eastern Canada and northeastern USA, *in* Stein, S., and Mazzotti, S., eds., Continental Intraplate Earthquakes: Science, Hazard, and Policy Issues: Geological Society of America Special Paper 425, p. 113–128, doi:10.1130/2007.9425(09).

Zoback, M.D., and Townend, J., 2001, Implications of hydrostatic pore pressures and high crustal strength for the deformation of intraplate lithosphere: Tectonophysics, v. 336, p. 19–30, doi: 10.1016/S0040-1951(01)00091-9.

Zoback, M.D., and Zoback, M.L., 1991, Tectonic stress field of North America and relative plate motion, *in* Slemmon, B., et al., eds., The Geology of North America, Decade Map Volume 1, Neotectonics of North America: Boulder, Colorado, Geological Society of America, p. 339–366.

Zoback, M.L., 1992a, First- and second-order patterns of stress in the lithosphere: The World Stress Map Project: Journal of Geophysical Research, v. 97, no. B8, p. 11,703–11,728, doi: 10.1029/92JB00132.

Zoback, M.L., 1992b, Stress field constraints on intraplate seismicity in eastern North America: Journal of Geophysical Research, v. 97, no. B8, p. 11,761–11,782, doi: 10.1029/92JB00221.

Zoback, M.L., and Richardson, R.M., 1996, Stress perturbation associated with the Amazonas and other ancient continental rifts: Journal of Geophysical Research, v. 101, no. B3, p. 5459–5475, doi: 10.1029/95JB03256.

Zoback, M.L., and Zoback, M.D., 1980, State of stress of the conterminous United States: Journal of Geophysical Research, v. 85, no. B8, p. 6113–6156, doi: 10.1029/JB085iB11p06113.

MANUSCRIPT RECEIVED 11 JUNE 2009
REVISED MANUSCRIPT RECEIVED 7 OCTOBER 2009
MANUSCRIPT ACCEPTED 14 OCTOBER 2009

Printed in the USA